J|A|C|S COMMUNICATIONS

Published on Web 09/15/2009

Periodic Mesoporous Organosilica with a Hexagonally Pillared Lamellar Structure

Hyung Ik Lee,[†] Ji Man Kim,*[,‡] and Galen D. Stucky*[,†]

Department of Chemistry and Biochemistry, University of California, Santa Barbara, California 93106, and Department of Chemistry, BK21 School of Chemical Materials Science, Department of Energy Science and SKKU Advanced Institute of Nanotechnology, Sungkyunkwan University, Suwon 440-746, Korea

Received June 25, 2009; E-mail: jimankim@skku.edu; stucky@chem.ucsb.edu

Historically, attempts to directly synthesize *pillared lamellar structures*[1] with sustainable and desirable large (>1 nm) pores, which had been previously obtained by postintercalation of pillaring agents, resulted in the discovery of a new family of ordered mesoporous materials (OMMs) formed via phase transitions from lamellar to sustainable periodic mesoporous structures.[2,3] Considerable additional research has resulted in OMMs with various additional mesostructures and a wide range of potential applications.[2−17] However, contrary to the early hypotheses concerning direct synthetic pillaring of a layered structure, the pillared OMM lamellar structure with a definable 3D periodic structure has not been accomplished to date.[18] Currently, three other types of more kinetically and thermodynamically accessible pore structures of OMMs, i.e., (i) columnar (2D hexagonal),[2−9] (ii) bi- or multicontinuous,[3,4,9−13] and (iii) discontinuous[4,8,9,14−17] mesostructures as defined from the perspective of the micelle (or pore) geometry, along with their respective subordinate symmetries have been successfully reported (Table S1 in the Supporting Information). The pillared lamellar structure, which, on the other hand, has been mathematically predicted as a *lamellar catenoid surface*[19] and recently found to exist as *mesh* and *perforated lamellar* structures in the research fields of surfactant and multiblock-copolymer mesophases,[20−22] still remains a mesostructure that has not been observed as an OMM for any specific symmetry (Table S1).

Here we report for the first time the synthesis of a 2D cylindrical type of mesoporous material with a *h*exagonally *p*illared *l*amellar (*HPL*) structure via phase transformation from a lamellar mesostructure. For the formation of the *HPL* mesostructure, a designed Gemini surfactant, $[C_nH_{2n+1}N(CH_3)_2(CH_2)_sN(CH_3)_2C_nH_{2n+1}]Br_2$ (designated as Gem_{n-s-n}, where $n = 16$ and $s = 3$ in the present work) was utilized as a structure-directing agent in the presence of the organosilica precursor 1,2-bis(triethoxysilyl)ethane (BTEE). In comparison with the corresponding monovalent surfactants, Gemini surfactants are a particularly interesting class of amphiphilic dimeric molecules with controllable hydrophobic tails and a spacer group that enable systematic variation of the headgroup charge density and micelle packing parameter g ($=V/a_0l$, where V is the total surfactant tail volume, a_0 is the effective surface headgroup area, and l is the kinetic surfactant tail length).[16,23] For the formation of the *HPL* mesophase, the organosilica dimeric precursor expands the range of hydrolysis/condensation rates and charge densities beyond those accessible by pure silica precursors such as tetraethylorthosilicate. The present *G*emini surfactant-templated periodic *m*esoporous *o*rganosilica with *HPL* mesostructure (designated as GMO-*HPL*) possesses a unique layered structure propped by hexagonally arrayed pillars and the consequent 2D cylindrical mesopores that independently run between the layers. GMO-*HPL* also has advantages for applications that use the hybrid framework composition to define the framework properties, including hydrothermal stability and surface functionality, as is well-demonstrated by previous reports.[24−27] During our preparation of this manuscript, Wiesner's group reported a *hexagonally patterned lamellar* mesophase of a triblock copolymer/aluminosilicate nanocomposite[28] whose *patterned* (perforated) *lamellar* structure of the aluminosilicate framework lacked pillars between layers, resulting in collapse of the structure. This is similar to the inverse replica of our mesoporous GMO-*HPL* material.

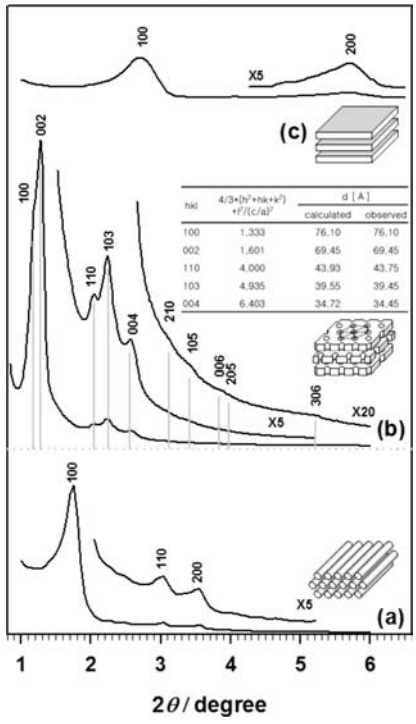

Figure 1. XRD patterns for (a) GMO-*H* and (b) GMO-*HPL* after surfactant extraction and (c) an as-made sample of GMO-*L*.

The pore structures of our GMO materials were verified by the complementary combination of X-ray diffraction (XRD), transmission electron microscopy (TEM), nitrogen sorption, and carbon replication. Figure 1 exhibits XRD patterns of GMO materials synthesized with different $Gem_{16-3-16}$/BTEE molar ratios ($x = 0.02-0.18$) followed by optional hydrothermal treatment at 373 K for 24 h (see the Supporting Information for details). When the concentration of Gemini surfactant was relatively low ($x = 0.02$) and hydrothermal treatment was applied, the XRD pattern showed three peaks, which can be indexed as (100), (110), and (200) for a typical 2D hexagonal mesostructure (Figure 1a).[2−6] This GMO

[†] University of California, Santa Barbara.
[‡] Sungkyunkwan University.

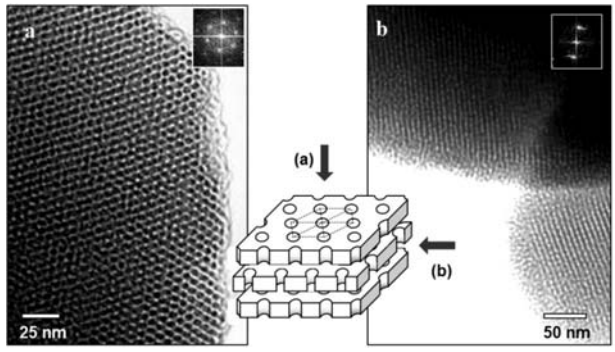

Figure 2. TEM images and (insets) ED patterns of the GMO-*HPL* material obtained from different directions: (a) perpendicular to the layers and (b) parallel to the layers. The schematic structure between the TEM images presents the surfactant mesophase in GMO-*HPL*.

material with a 2D *h*exagonal mesostructure (*p*6*mm*) is designated as GMO-*H*. At a much higher concentration of surfactant ($x = 0.18$) with hydrothermal treatment, a new mesostructure (GMO-*HPL*) was obtained, as shown in Figure 1b. GMO-*HPL* gave a total of ten diffraction peaks (five intense, well-resolved peaks and five additional weak peaks), which can be definitively indexed as the (100), (002), (110), (103), (004), (210), (105), (006), (205), and (306) reflections of a 3D hexagonal system ($a = 8.79$ nm and $c = 13.89$ nm, based on space group $P6_3/mmc$ with ABAB stacking).[4,16,17] For clarity, XRD peaks calculated according to the $P6_3/mmc$ symmetry are displayed as gray bars along with the experimentally obtained XRD result (Figure 1b) and also summarized in the inset of Figure 1b. All of the experimental XRD peaks are in excellent agreement with the calculated peak positions and exhibit a very small error range of less than 0.8% in the *d*-spacing values. In the absence of hydrothermal treatment ($x = 0.18$), an XRD pattern typical of a lamellar mesostructure (designated as GMO-*L*) was obtained, as shown in Figure 1c. The XRD peaks of GMO-*L* disappeared after the removal of the surfactant by solvent extraction because of structural collapse, which is consistent with previous reports.[9,29]

Figure 2 exhibits TEM images and electron diffraction (ED) patterns for the GMO-*HPL* material. As illustrated in the schematic diagram in Figure 2, the TEM images were taken from different directions of the incident electron beam, i.e., (a) perpendicular and (b) parallel to the perforated layers. The schematic diagram represents the assembled Gemini surfactant mesophase that would create the void pores of the GMO-*HPL* structure after removal of the surfactant. Figure 2a shows hexagonally arrayed dark spots, which originate from the pillaring framework components between the layers (hexagonally arrayed holes in the schematic diagram). These hexagonal pillars appear to be formed by the infiltration of framework species within the perforated spaces of the surfactant micelle layers under the present synthesis conditions [high concentration of $Gem_{16-3-16}$ ($x = 0.18$) and hydrothermal treatment at 100 °C]. The TEM image in Figure 2b, obtained from the parallel direction, clearly indicates that the GMO-*HPL* material is basically made of lamellar structures with pillars. The wide uniform areas in the TEM images and ED patterns (insets of Figure 2a,b) from the two directions, along with XRD patterns in Figure 1b, are suggestive of excellent long-range 3D order in the GMO-*HPL* material. The unit cell parameters, estimated from the TEM images, are $a = 8.75$ nm and $c = 13.4$ nm, which also correspond well with the values obtained from the XRD pattern (Figure 1b).

The N_2 adsorption−desorption isotherms in Figure 3 were obtained in order to substantiate the uniformity of the mesoporous structures. The GMO-*H* and GMO-*HPL* materials exhibited typical

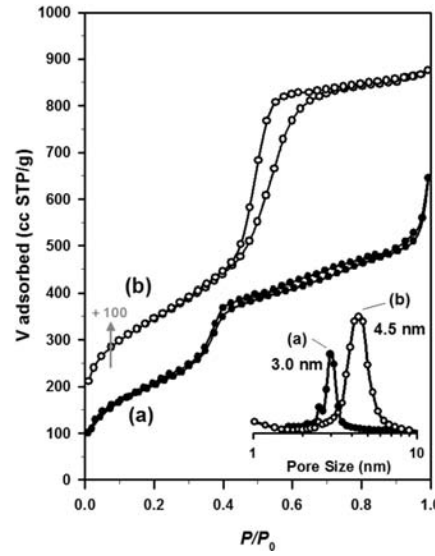

Figure 3. N_2 adsorption−desorption isotherms obtained from (a) GMO-*H* and (b) GMO-*HPL* at liquid N_2 temperature and (inset) the corresponding BJH pore size distribution curves from the adsorption branches.

type-IV isotherms with steep capillary condensation steps in the P/P_0 ranges 0.35−0.4 and 0.50−0.60, respectively, confirming that both materials have highly uniform and well-developed mesopores. The isotherm patterns with no or narrow hysteresis loops are indicative of the cylindrical or continuous pore structures of GMO-*H* and GMO-*HPL* materials, which are significantly different from the cage-type pore structure with a wide H_2 hysteresis loop.[30] The pore size distribution curves were obtained from the adsorption branches using the Barrett−Joyner−Halenda (BJH) method[31] (inset of Figure 3). The pore size and specific surface area of GMO-*HPL* were 4.5 nm and 922 m^2/g, respectively, which are relatively larger and higher than those of GMO-*H* (3.0 nm and 767 m^2/g, respectively). The uniformity of the mesopore size in GMO-HPL also supports the fact that the previously shown XRD peaks of the GMO-*HPL* material (Figure 1b) are from a pure mesophase and not from a mixture of different materials that accidentally matches the $P6_3/mmc$ space group.

On the basis of the XRD results in Figure 1b,c, it seems that the lamellar mesophase is initially formed at 298 K and transformed to the *HPL* mesostructure during the hydrothermal treatment at 373 K for 24 h. This speculation is consistent with a *charge density matching model*, in which the lamellar mesophases continuously transform to a 2D hexagonal cylindrical mesophase via the change of charge density of the silica species during their condensation reaction in the hydrothermal reaction.[32] However, in our synthesis system, the lamellar mesophase is transformed not to the 2D hexagonal mesophase but to an intermediate phase, the *HPL* mesophase, which is made accessible by the nature of the $Gem_{16-3-16}$ surfactant and the organosilica precursor.

In order to better confirm the present mesostructure, we also used the GMO-*HPL* material as a rigid template to obtain an inversely replicated carbon material via a nanoreplication method reported elsewhere.[33] Figure 4 shows scanning electron microscopy (SEM) images of the GMO-*HPL* and carbon replica materials. The morphology of the carbon replica material (Figure 4b) is similar to that of the GMO-*HPL* template (Figure 4a), but the overall thickness of the particles is considerably contracted, which might be due to the asymmetric structural collapse of the lamellar-based carbon replica without pillars. The high-resolution SEM image in Figure 4c clearly indicates that the carbon replica material is made up of

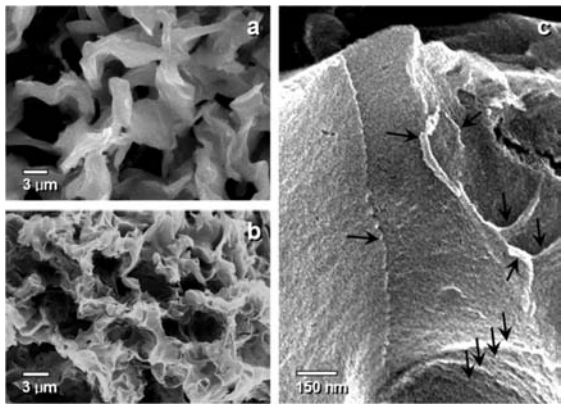

Figure 4. SEM images of (a) GMO-*HPL* material, (b) a carbon replica of GMO-*HPL*, and (c) a high-resolution SEM image of the carbon replica. Arrows indicate revealed edges of lamellar structures of the carbon replica.

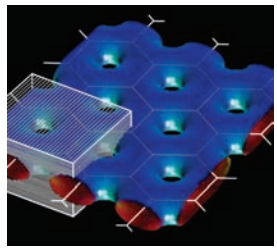

Figure 5. 2D structure of the lamella catenoid surface.[19] The lamellas are stacked to form a 3D periodic structure. The added white box and lines display the organosilica framework and the surfactant (or pore) channel structures, respectively, for GMO-*HPL*.

ultrathin nanosheets after the removal of the organosilica frameworks. The nanosheets were observed to peel from the carbon-sheet bundles during the SEM measurement. These bundles of sheet-like structures in Figure 4c appear to be very similar to the hexagonally perforated mesophase of the surfactant or polymer system illustrated in Figure 2. The structure of the carbon replica material confirms the mesoporous structure of the GMO-*HPL* material.

In summary, we have reported the synthesis of a new type of ordered mesoporous material with a hexagonally pillared lamellar mesostructure (GMO-*HPL*) based on a lamellar catenoid surface (Figure 5). It has been demonstrated that the *HPL* phase, which has been predicted by theory to be a highly unstable intermediate mesophase,[19−22] can be obtained as a real OMM via phase transformation from a lamellar mesophase by hydrothermal reaction of an organosilica precursor in the presence of a high concentration of a designed Gemini surfactant ($Gem_{16-3-16}$) that has a large g value. The present GMO-*HPL* material provides a fascinating topological link between lamellar and 2D hexagonal mesophases. The unique 3D periodicity with two-dimensionally connected pore channels that run between the framework layers of GMO-*HPL* may be especially useful in applications that require selective 2D diffusion in different directions. Moreover, the present synthesis strategy based on the synergetic assembly of a designed Gemini surfactant and an organosilica precursor may be beneficial for the further synthesis and use of other hard-to-access mesophases.

Acknowledgment. This work was supported by the Korea Science and Engineering Foundation funded by the Ministry of Education, Science and Technology (World Class University Program, R31-2008-000-10029-0) and the Korea Research Foundation (University Professor Overseas Visiting Research Support Project, KRF-2008-013-C00050). Partial support for this research was provided by Corning, Inc.

Supporting Information Available: Table of hitherto-reported mesophases, experimental methods, and table of physicochemical properties of materials. This material is available free of charge via the Internet at http://pubs.acs.org.

References

(1) Pinnavaia, T. J. *Science* **1983**, *220*, 365–371.
(2) Yanagisawa, T.; Shimizu, T.; Kuroda, K.; Kato, C. *Bull. Chem. Soc. Jpn.* **1990**, *63*, 988–992.
(3) Kresge, C. T.; Leonowicz, M. E.; Roth, W. J.; Vartuli, J. C.; Beck, J. S. *Nature* **1992**, *359*, 710–712.
(4) Huo, Q. S.; Margolese, D. I.; Stucky, G. D. *Chem. Mater.* **1996**, *8*, 1147–1160.
(5) Kim, S. S.; Pauly, T. R.; Pinnavaia, T. J. *Chem. Commun.* **2000**, 1661–1662.
(6) Zhao, D. Y.; Feng, J. L.; Huo, Q. S.; Melosh, N.; Fredrickson, G. H.; Chmelka, B. F.; Stucky, G. D. *Science* **1998**, *279*, 548–552.
(7) Zhao, D. Y.; Huo, Q. S.; Feng, J. L.; Kim, J. M.; Han, Y. J.; Stucky, G. D. *Chem. Mater.* **1999**, *11*, 2668–2672.
(8) Kim, J. M.; Sakamoto, Y.; Hwang, Y. K.; Kwon, Y. U.; Terasaki, O.; Park, S. E.; Stucky, G. D. *J. Phys. Chem. B* **2002**, *106*, 2552–2558.
(9) Wan, Y.; Zhao, D. Y. *Chem. Rev.* **2007**, *107*, 2821–2860.
(10) Kleitz, F.; Choi, S. H.; Ryoo, R. *Chem. Commun.* **2003**, 2136–2137.
(11) Jain, A.; Toombes, G. E. S.; Hall, L. M.; Mahajan, S.; Garcia, C. B. W.; Probst, W.; Gruner, S. M.; Wiesner, U. *Angew. Chem., Int. Ed.* **2005**, *44*, 1226–1229.
(12) Gao, C. B.; Sakamoto, Y.; Sakamoto, K.; Terasaki, O.; Che, S. N. *Angew. Chem., Int. Ed.* **2006**, *45*, 4295–4298.
(13) Han, Y.; Zhang, D.; Chng, L. L.; Sun, J.; Zhao, L.; Zou, X.; Ying, J. Y. *Nat. Chem.* **2009**, *1*, 123–127.
(14) Huo, Q. S.; Margolese, D. I.; Ciesla, U.; Feng, P. Y.; Gier, T. E.; Sieger, P.; Leon, R.; Petroff, P. M.; Schuth, F.; Stucky, G. D. *Nature* **1994**, *368*, 317–321.
(15) Sakamoto, Y.; Kaneda, M.; Terasaki, O.; Zhao, D. Y.; Kim, J. M.; Stucky, G.; Shim, H. J.; Ryoo, R. *Nature* **2000**, *408*, 449–453.
(16) Huo, Q. S.; Leon, R.; Petroff, P. M.; Stucky, G. D. *Science* **1995**, *268*, 1324–1327.
(17) Sakamoto, Y.; Diaz, I.; Terasaki, O.; Zhao, D. Y.; Perez-Pariente, J.; Kim, J. M.; Stucky, G. D. *J. Phys. Chem. B* **2002**, *106*, 3118–3123.
(18) Kim, S. S.; Zhang, W. Z.; Pinnavaia, T. J. *Science* **1998**, *282*, 1302–1305.
(19) Abundant informative visualizations and mathematical elucidations of phases are available at http://www.msri.org/publications/sgp/SGP/.
(20) Hyde, S. T.; Schroder, G. E. *Curr. Opin. Colloid Interface Sci.* **2003**, *8*, 5–14.
(21) Hamley, I. W.; Koppi, K. A.; Rosedale, J. H.; Bates, F. S.; Almdal, K.; Mortensen, K. *Macromolecules* **1993**, *26*, 5959–5970.
(22) Ludwigs, S.; Boker, A.; Voronov, A.; Rehse, N.; Magerle, R.; Krausch, G. *Nat. Mater.* **2003**, *2*, 744–747.
(23) Alami, E.; Beinert, G.; Marie, P.; Zana, R. *Langmuir* **1993**, *9*, 1465–1467.
(24) Inangki, S.; Guan, S.; Fukushima, Y.; Ohsuna, T.; Terasaki, O. *J. Am. Chem. Soc.* **1999**, *121*, 9611–9614.
(25) Asefa, T.; MacLachlan, M. J.; Coombs, N.; Ozin, G. A. *Nature* **1999**, *402*, 867–871.
(26) Melde, B. J.; Holland, B. T.; Blanford, C. F.; Stein, A. *Chem. Mater.* **1999**, *11*, 3302–3308.
(27) Haton, B.; Landskron, W. W.; Perovic, D.; Ozin, G. A. *Acc. Chem. Res.* **2005**, *38*, 305–312.
(28) Toombes, G. E. S.; Mahajan, S.; Thomas, M.; Du, P.; Tate, M. W.; Gruner, S. M.; Wiesner, U. *Chem. Mater.* **2008**, *20*, 3278–3287.
(29) Holmqvist, P.; Alexandridis, P.; Lindman, B. *J. Phys. Chem. B* **1998**, *102*, 1149–1158.
(30) Matos, J. R.; Kruk, M.; Mercuri, L. P.; Jaroniec, M.; Zhao, L.; Kamiyama, T.; Terasaki, O.; Pinnavaia, T. J.; Liu, Y. *J. Am. Chem. Soc.* **2003**, *125*, 821–829.
(31) Barrett, E. P.; Joyner, L. G.; Halenda, P. P. *J. Am. Chem. Soc.* **1951**, *73*, 373–380.
(32) Firouzi, A.; Kumar, D.; Bull, L. M.; Besier, T.; Sieger, P.; Huo, Q.; Walker, S. A.; Zasadzinski, J. A.; Glinka, C.; Nicol, J.; Margolese, D.; Stucky, G. D.; Chmelka, B. F. *Science* **1995**, *267*, 1138–1143.
(33) Ryoo, R.; Joo, S. H.; Jun, S. *J. Phys. Chem. B* **1999**, *103*, 7743–7746.

JA905245U